Oncogene (2016) **35,** 3796–3806

www.nature.com/onc

OPEN

ORIGINAL ARTICLE

Heterozygous *PALB2* c.1592delT mutation channels DNA double-strand break repair into error-prone pathways in breast cancer patients

K Obermeier[1,6], J Sachsenweger[1,6], TWP Friedl[1], H Pospiech[2,3], R Winqvist[4,5,7] and L Wiesmüller[1,7]

Hereditary heterozygous mutations in a variety of DNA double-strand break (DSB) repair genes have been associated with increased breast cancer risk. In the Finnish population, *PALB2* (partner and localizer of BRCA2) represents a major susceptibility gene for female breast cancer, and so far, only one mutation has been described, c.1592delT, which leads to a sixfold increased disease risk. PALB2 is thought to participate in homologous recombination (HR). However, the effect of the Finnish founder mutation on DSB repair has not been investigated. In the current study, we used a panel of lymphoblastoid cell lines (LCLs) derived from seven heterozygous female *PALB2* c.1592delT mutation carriers with variable health status and six wild-type matched controls. The results of our DSB repair analysis showed that the *PALB2* mutation causes specific changes in pathway usage, namely increases in error-prone single-strand annealing (SSA) and microhomology-mediated end-joining (MMEJ) compared with wild-type LCLs. These data indicated haploinsufficiency regarding the suppression of error-prone DSB repair in *PALB2* mutation carriers. To the contrary, neither reduced HR activities, nor impaired RAD51 filament assembly, nor sensitization to PARP inhibition were consistently observed. Expression of truncated mutant versus wild-type PALB2 verified a causal role of *PALB2* c.1592delT in the shift to error-prone repair. Discrimination between healthy and malignancy-presenting *PALB2* mutation carriers revealed a pathway shift particularly in the breast cancer patients, suggesting interaction of *PALB2* c.1592delT with additional genomic lesions. Interestingly, the studied *PALB2* mutation was associated with 53BP1 accumulation in the healthy mutation carriers but not the patients, and 53BP1 was limiting for error-prone MMEJ in patients but not in healthy carriers. Our study identified a rise in error-prone DSB repair as a potential threat to genomic integrity in heterozygous *PALB2* mutation carriers. The used phenotypic marker system has the capacity to capture dysfunction caused by polygenic mechanisms and therefore offers new strategies of cancer risk prediction.

Oncogene (2016) **35,** 3796–3806; doi:10.1038/onc.2015.448; published online 7 December 2015

INTRODUCTION

Hereditary mutations in a variety of genes involved in double-strand break (DSB) repair are associated with an increased risk of developing female breast cancer.[1–6] However, only a fraction of approximately 30% of this hereditary cancer risk is explained by currently known high-penetrance susceptibility genes. A large portion of the remaining predisposition to breast cancer may be explained by a polygenic model involving a combination of multiple genomic risk factors, including the effect of low-penetrance susceptibility alleles. These include polymorphisms in genes involved in several metabolic pathways, signal transduction and DNA repair.[7]

In the Finnish population, *PALB2* was reported to represent the most notable breast cancer susceptibility gene[8] along with the previously identified *BRCA1* and *BRCA2* genes. Interestingly, there is only one single aberration in *PALB2* described in this population so far, namely the relatively common c.1592delT protein truncation founder mutation. In females, this mutation leads to a sixfold increase of the breast cancer risk[9] and occurs in 0.2% of the general population.[10] Several investigations have now shown that monoallelic mutations in *PALB2* increase the risk of developing female breast cancer,[8,11,12] whereas biallelic mutations cause *Fanconi anemia* (FA) of subtype FA-N.[13–15] A hallmark of FA patient cells is defectiveness in interstrand crosslink repair, a feature that is being made use of in diagnostic patient classification.[16]

DNA strand breaks, particularly DSBs, are the most lethal genomic lesions. In mammalian cells, DSBs are repaired by two main pathways: non-homologous end-joining (NHEJ) and homologous recombination (HR).[17] DSBs generated during crosslink repair are normally subject to HR repair.[16,18] HR starts with processing of the DNA end, thereby forming single-stranded DNA (ssDNA) 3′ends, which are quickly covered by the human ssDNA-binding protein RPA. DNA end processing involves the MRE11-RAD50-Nibrin and BRCA1-CtIP complexes. PALB2 acts as the mediator between BRCA1 and BRCA2 via independent interactions at its N- and C-terminus, respectively.[19–22] The C-terminus

[1]Department of Obstetrics and Gynecology, Ulm University, Ulm, Germany; [2]Faculty of Biochemistry and Molecular Medicine, University of Oulu, Oulu, Finland; [3]Research Group Biochemistry, Leibniz Institute for Age Research-Fritz Lipmann Institute, Jena, Germany; [4]Laboratory of Cancer Genetics and Tumor Biology, Cancer and Translational Medical Research Unit and Biocenter Oulu, University of Oulu, Oulu, Finland and [5]Northern Finland Laboratory Centre NordLab, Oulu, Finland. Correspondence: Professor R Winqvist, Laboratory of Cancer Genetics and Tumor Biology, Cancer and Translational Medical Research Unit and Biocenter Oulu, University of Oulu, Aapistie 5A, 90220 Oulu, Finland or Professor L Wiesmüller, Department of Obstetrics and Gynecology, Ulm University, Prittwitzstrasse 43, Ulm 89075, Germany.
E-mail: robert.winqvist@oulu.fi or lisa.wiesmueller@uni-ulm.de
[6]These authors shared first authorship.
[7]These authors shared senior authorship.
Received 19 February 2015; revised 29 September 2015; accepted 15 October 2015; published online 7 December 2015

additionally binds RAD51C, another breast/ovarian cancer susceptibility as well as FA gene product, thus forming a HR complex also containing XRCC3 and RAD51.[23] BRCA1 may concentrate PALB2 at DNA damage sites in chromatin,[20,21] where PALB2 recruits and permits stable localization of BRCA2 to these focal intranuclear sites.[19,24,25] BRCA2 promotes the assembly of RAD51 into nucleoprotein filaments thereby replacing RPA.[26,27] RAD51 nucleoprotein filaments invade the sister chromatid in search for homology. This represents the central step of HR. It either starts repair synthesis during the unilateral exchange process called synthesis-dependent strand annealing or formation of double Holliday Junctions, which are later resolved in a crossover or non-crossover manner during canonical HR.[17] PALB2 has also been reported to bind to ssDNA where it interacts with RAD51 to stimulate strand invasion.[28] Importantly, similar HR-related processes that require PALB2, BRCA2 and RAD51 have also a central role in the reactivation of stalled replication forks.[29–33] Altogether, PALB2 has been described to exhibit indirect and direct functions in RAD51-dependent HR, which is considered to be the most accurate DSB repair pathway. High fidelity repair by HR requires perfect homologies between the donor and the acceptor sequence, which is why it takes place in the S/G2-phase, when identical sister chromatids are available.[34] For comparison, NHEJ, in particular the alternative microhomology-mediated end-joining (MMEJ) sub-pathway, and an alternative RAD51-independent homologous DSB repair pathway, namely single-strand annealing (SSA), are error-prone DSB repair mechanisms that are not limited to a particular cell cycle phase.[34,35] NHEJ can result in the loss or gain of nucleotides and hence in the disruption of genomic integrity. Similarly, SSA starts with DNA end processing, however, followed by DNA annealing between genomic repeat sequences with extensive homologies. SSA always leads to the loss of the intervening DNA sequences and, therefore, is considered mutagenic.[35]

In a previous study, we observed enhanced error-prone DSB repair activities, namely MMEJ and SSA, in lymphoblastoid cell lines (LCLs) from *BRCA1* and *BRCA2* mutation carriers, respectively.[36] As PALB2 was discovered to physically connect BRCA1 and BRCA2,[19–21] we mechanistically dissected DSB repair activities in LCLs derived from female individuals heterozygous for the Finnish *PALB2* c.1592delT founder mutation. The breast cancer risks associated with *PALB2* mutations have been reported to synergize with additional genetic factors.[37,38] To better understand the impact of polygenic interactions with the Finnish founder mutation on cancer risk-associated DSB repair dysfunction, we compared cohorts with and without *PALB2* c.1592delT mutation and with and without breast cancer. The data presented in this study demonstrate that mutated *PALB2* derepresses SSA and MMEJ, a phenotype which very likely cooperates with additional changes in carrier individuals with cancer, such as deregulation of 53BP1 levels associated with the lack of protection against excessive end processing.

RESULTS

Individuals heterozygous for the Finnish *PALB2* founder mutation show specific changes in DSB repair pathway usage

To determine whether and how DSB repair is altered in individuals heterozygous for the Finnish c.1592delT *PALB2* founder mutation, we introduced different *EGFP*-based reporter constructs into LCLs from *PALB2* mutation carriers and healthy individuals with wild-type *PALB2*[32,39] (Supplementary Table 1). Our systematic analysis of pathway-specific DSB repair activities addressed NHEJ, MMEJ, SSA, SSA+HR and HR (Figures 1a and b and representative FACS plots in Supplementary Figure 1), where *PALB2* wild-type LCL BR-0968 served as internal reference. As summarized in Table 1, we observed statistically significant increases in NHEJ (1.5- to 3.4-fold), MMEJ (1.8- to 9.6-fold), SSA (1.6- to 7.9-fold) and/or SSA+HR (1.8- to 10.9-fold) in five LCLs from *PALB2* mutation carriers, encompassing individuals without (healthy) and with breast cancer (brca). However, in LCL BR-0970 from a breast cancer patient undergoing cytostatic therapy (brca+therapy), no such increases were observed, rather a reduction such as for SSA+HR (to 70%). As the only other exception, significant downregulation of SSA (to 60%) was found in LCL BR-0724 (brca). Regarding HR, we obtained no statistically significant changes in *PALB2*-mutated LCLs, except for BR-0970 (brca+therapy) displaying HR downregulation to 20%. Notably, BR-0970 cells from the breast cancer patient undergoing therapy were the only ones that did not match any of the DSB repair changes observed with the other LCLs from *PALB2* mutation carriers and were therefore excluded from any cohort analysis in this work. Accordingly, augmentation of NHEJ, MMEJ, SSA and SSA+HR was detected in 83% (5/6) of *PALB2*-mutated LCLs. In conclusion, DSB repair analysis of individual LCLs revealed a shift to error-prone DSB repair pathways in *PALB2* mutation carriers with and without breast cancer before therapy.

To take the possibility into account that the internal reference BR-0968 may not perfectly represent the wild-type phenotype, we performed cohort analysis for the informative pathways NHEJ, MMEJ, SSA and SSA+HR. Thus, we calculated mean values of specific DSB repair activities from six *PALB2*-mutated LCLs (excluding BR-0970 from the patient undergoing therapy) and six matched LCLs with wild-type *PALB2* (for individual analysis of LCLs see Table 1). When comparing the two different genotypes, no statistically significant change in NHEJ was observed. However, the mutation carriers showed a 1.8-fold increase in MMEJ ($P = 0.022$) and SSA ($P = 0.001$) and a 1.9-fold increase in SSA+HR ($P = 0.002$) in relation to the wild-type cohort (Figure 2a, left panel). Moreover, plotting MMEJ changes in *PALB2*-mutated LCLs (Table 1) against the respective PALB2 protein levels according to our previous study[32] revealed a statistically significant inverse correlation ($P = 0.0167$; Spearman r, two-tailed). When subdividing the group of *PALB2*-mutated LCLs, we noticed a statistically significant 2.0-fold NHEJ increase in the breast cancer patients compared with healthy *PALB2*-mutated donors ($P = 0.005$) (Figure 2a, right panel). No statistically significant MMEJ differences were observed between the subgroups. Furthermore, the breast cancer patients showed a 2.2-fold increase in SSA ($P = 0.0034$) and a 2.0-fold increase in SSA+HR ($P = 0.003$) compared with the wild-type LCLs. Under the transient assay conditions applied to patient cells, analysis of SSA+HR was previously found to primarily reflect SSA activities, so that the SSA +HR data further supported increased usage of this pathway.[40,41] In summary, cohort analysis confirmed MMEJ and SSA upregulation in *PALB2* c.1592delT mutation carriers versus wild-type controls. When subdividing the group of mutation carriers into healthy and breast cancer-affected individuals, we found a difference only for NHEJ, namely a rise in those with breast cancer. The same subgroup also showed elevated SSA versus the wild-type cohort (not healthy mutation carriers versus the wild-type cohort). Surprisingly, overexpression of wild-type PALB2 did not affect SSA+HR in carriers or wild-type control LCLs (Figure 2b). Instead overexpression of the truncated PALB2 encoded by *PALB2* c.1592delT caused a 1.6- and 1.5-fold increase in SSA+HR ($P < 0.0001$).

Heterozygously mutated *PALB2* rarely associates with sensitivity to PARP inhibitor treatment

Following the detection of ssDNA breaks, poly(ADP-ribosyl) transferase (PARP)1–3 activate various DNA repair pathways and stabilize stalled replication forks.[42] Resolution of stalled forks requires HR, that is, the pathway PALB2 is thought to have a role in.[32] PARP inhibition was shown to eliminate *BRCA1*- and

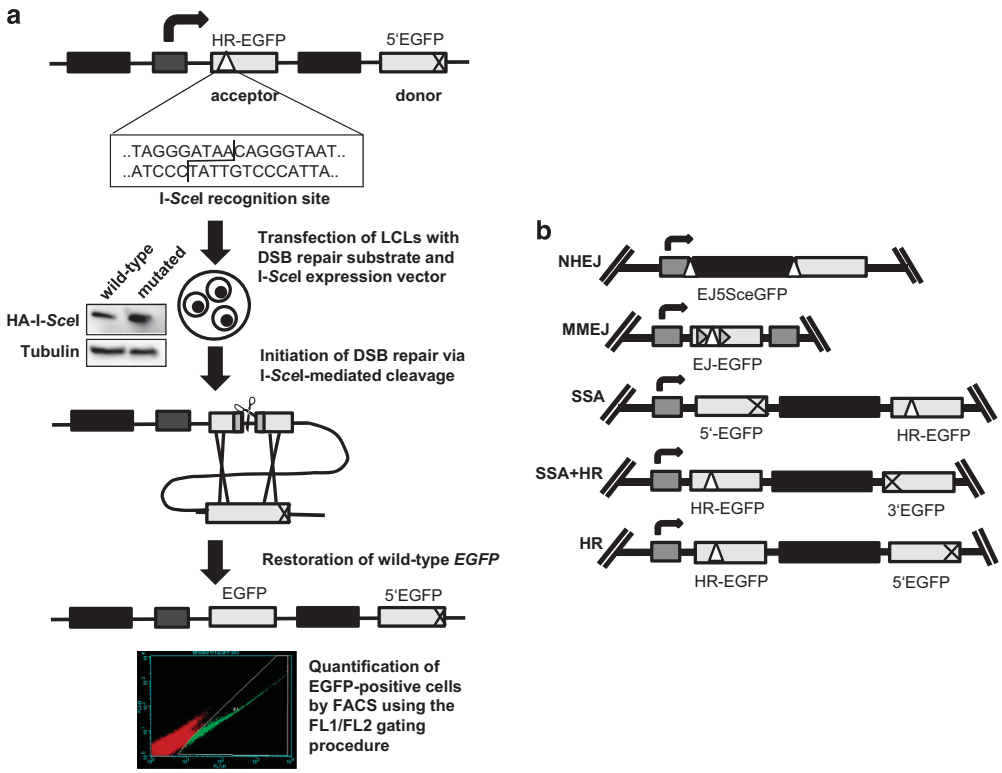

Figure 1. Assay for comparison of DSB repair pathway usage in individuals with wild-type and heterozygously mutated *PALB2*. (**a**) Assay principle for the analysis of DSB repair pathways in LCLs.[39] Representatively shown is the construct enabling HR between a mutated *EGFP*-acceptor sequence with an I-*Sce*I recognition site and a donor sequence representing truncated *EGFP*. A plasmid mixture, containing the DSB repair substrate HR-EGFP/5'EGFP, I-*Sce*I-meganuclease expression plasmid (pCMV-I-*Sce*I), and either filler plasmid pBS or wild-type *EGFP* expression plasmid were introduced into the LCLs by electroporation followed by cultivation for 48 h. DSB repair was triggered by I-*Sce*I-mediated DSB formation followed by the restoration of *EGFP* and appearance of green fluorescent cells which were analyzed flow cytometrically. As proof-of-principle, BR-0968 and BR-0967 cells with wild-type and heterozygously mutated *PALB2* were transfected according to the protocol and cells harvested 24 h later. Expression of the HA-I-*Sce*I fusion protein was verified by immunoblotting with antibody directed against the HA-tag. Transfection efficiencies were determined for each sample and used to individually normalize DSB repair frequencies thereby excluding potential frequency changes related to transfection, transcription, translation, proliferation and lethality. (**b**) Constructs for specific DSB repair analysis. Constructs for the assessment of different DSB repair pathways are shown: NHEJ (EJ5SceGFP), MMEJ (EJ-EGFP), SSA (5'EGFP/HR-EGFP), SSA+HR (HR-EGFP/3'EGFP) and HR (HR-EGFP/5'EGFP). The NHEJ substrate contains two I-*Sce*I recognition sites. Mutated *EGFP* genes, light gray boxes; deleted *EGFP* sequence, cross; I-*Sce*I recognition site, white triangle; microhomologies, gray triangles; promoter sequence, gray box; spacer sequence, black box.

BRCA2-mutated tumor cells in preclinical and clinical studies.[43] As PALB2 physically and functionally interacts with BRCA1 and BRCA2,[19–22] sensitivity to PARP inhibition was assessed in the *PALB2*-mutated LCLs. For this purpose, LCLs were treated with different concentrations of the PARP inhibitor 1,5-isoquinolinediol and subjected to MTT assay. As a proof-of-principle, we showed that this approach may detect HR dysfunction in a gene dose-dependent manner, because LCL cells with biallelic *BRCA2* mutation (GM13023A) showed 3.8-fold higher sensitivity ($P = 0.0138$) than heterozygously *BRCA2*-mutated (HA238) cells, that is, highest sensitivity compared with wild-type control cells (TK6) (Table 2). When analyzing *PALB2*-mutated LCLs, we observed statistically significantly reduced IC50 values for BR-0760 (brca) and BR-0970 (brca+therapy) versus the wild-type reference BR-0968. But none of the other five *PALB2*-mutated LCLs showed a significant increase of PARP inhibitor sensitivity. IC50 values of five additional LCLs with wild-type *PALB2* were also not significantly different from the wild-type reference BR-0968. Consistently, cohort analysis of LCLs from wild-type *PALB2* and *PALB2*-mutated donors with or without breast cancer revealed no differences between the mean IC50 values of the subgroups (Figure 3).

Analysis of DSB repair components reveals accumulation of 53BP1 in healthy *PALB2* mutation carriers

To further delineate the molecular defect caused by heterozygous *PALB2* mutation in DSB repair, we performed immunofluorescence microscopic analysis of nuclear structures indicative of the accumulation and/or removal of DSBs (53BP1) and the assembly/disassembly of the HR repair machinery (RAD51).[41] Depending on the selected genotoxic treatment, distinct DNA repair pathways can be addressed such as canonical NHEJ in the early repair phase after irradiation, HR after treatment with the crosslinker Mitomycin C (MMC).[16,18,34]

First, we induced DSBs in LCLs by exposure to ionizing radiation (2 Gy γ-ray) and subjected the cells to immunostaining and quantitative immunofluorescence microscopy at different time points post irradiation. Accumulation of 53BP1 0.5–1 h after ionizing radiation was followed by a gradual decrease of foci numbers indicating DSB formation and subsequent repair both in wild-type and *PALB2*-mutated LCLs (Supplementary Figure 2a). When monitoring RAD51 filament assembly post irradiation, we detected similar kinetics of foci accumulation and decline as with 53BP1 (Supplementary Figure 2b). A statistically significant difference in 53BP1 or RAD51 foci numbers specific for a

Table 1. DSB repair frequency changes in LCLs from *PALB2* mutation carriers and wild-type controls

Cell line	*PALB2 genotype*	*Health status*	*DSB repair frequency change: mean tested LCL versus mean wild-type control*[a] (P-*value*)[b]				
			NHEJ	*MMEJ*	*SSA*	*SSA+HR*	*HR*
BR-0954	c.1592delT/wt	Healthy	1.5 (0.0260)	1.8 (0.0028)	1.6 (0.0003)	1.8 (0.0078)	ns
BR-0967			ns[c]	3.4 (0.0022)	4.0 (0.0022)	3.5 (0.0022)	nd[d]
BR-0724		brca	2.7 (0.0022)	ns	0.6 (0.0043)	ns	nd
BR-0736			2.7 (0.0022)	9.6 (0.0022)	7.9 (0.0022)	10.9 (0.0022)	nd
BR-0737			3.4 (0.0022)	2.4 (0.0142)	1.8 (<0.0001)	2.0 (0.0019)	ns
BR-0760			2.1 (0.0087)	1.9 (0.0188)	3.5 (<0.0001)	3.8 (<0.0001)	ns
BR-0970		brca+ therapy	ns	ns	ns	0.7 (0.0028)	0.2 (0.0078)
BR-0778	Wild-type	Healthy	4.1 (0.0022)	1.4 (0.0260)	ns	2.0 (0.0043)	ns
BR-0781			1.9 (0.0043)	ns	ns	ns	ns
BR-1016			ns	ns	ns	ns	ns
BR-1017			1.9 (0.0022)	ns	5.3 (0.0022)	7.2 (0.0022)	nd
BR-1023			2.8 (0.0022)	ns	2.1 (0.0022)	1.8 (0.0022)	nd

Abbreviations: brca, breast cancer patient; brca+therapy, breast cancer patient undergoing cytostatic therapy; DSB, double-strand break; HR, homologous recombination; LCLs, lymphoblastoid cell lines; MMEJ, microhomology-mediated end-joining; NHEJ, non-homologous end-joining; SSA, single-strand annealing. LCLs were subjected to pathway-specific DSB repair measurements as described in the legend to Figure 1. Each *PALB2*-mutated LCL was analyzed parallel to the wild-type reference LCL BR-0968 and mean frequencies were set to 100%. Mean frequencies from at least six biological replicates were determined (replicate numbers for NHEJ/MMEJ/SSA/SSA+HR/HR: BR-0954 6/9/9/9/6, BR-0967 6/6/6/6/6, BR-0724 6/6/6/6/6, BR-0736 6/6/6/6/6, BR-0737 6/9/9/9/9, BR-0760 6/9/9/9/9, BR-0970 6/9/9/9/9, BR-0778 6/6/6/6/6, BR-0781 6/6/6/6/6, BR-1016 6/9/9/9/6, BR-1017 6/6/6/6/6, BR-1023 6/6/6/6/6, and reference BR-0968 18/36/33/36/24). Relative frequency changes between tested and reference LCLs were calculated. Statistically significant differences were calculated by Mann–Whitney test for unpaired samples. Note that HR measurements were not calculated for several LCLs (nd) because of transfection efficiencies $<10\%$, so that HR frequencies were close to the detection limit. [a]DSB repair frequency changes (x-fold) for tested LCLs in relation to wild-type control BR-0968 analyzed in parallel ($n=6$–9). [b]*P*-values were calculated by Mann–Whitney test for unpaired samples. [c]ns, statistically non-significant ($P>0.05$). [d]nd, not determined; note that HR measurements were not calculated for several LCLs (nd) because of transfection efficiencies $<10\%$, so that HR frequencies were close to the detection limit.

PALB2–mutated LCL versus the wild-type reference BR-0968 was only observed in one single case each (Supplementary Figure 1 and further data not shown). To focus on HR, we treated the LCLs with MMC inducing a gradual increase of 53BP1 foci numbers up to 6 h after exposure indicating DSB formation during crosslink processing.[41] MMC treatment did not unveil any difference in 53BP1 accumulation in individual LCLs (Supplementary Figure 2c). RPA coats ssDNA and becomes phosphorylated at the 32 kDa subunit (P-RPA) when accumulating on DNA.[44] P-RPA foci kinetics post ionizing radiation did not reveal differences between LCLs from family I members with wild-type or mutated *PALB2* (Supplementary Figure 2d). Cohort analysis of LCLs from wild-type and *PALB2*-mutated donors with or without breast cancer verified the increases in foci numbers for both treatment modalities and time points post treatment (Figure 4). It further demonstrated complete absence of significant differences between the subgroups (wild-type, *PALB2*-mutated and healthy, *PALB2*-mutated and breast cancer) regarding 53BP1 and RAD51 foci/nucleus before and after irradiation as well as 53BP1 foci/nucleus before and after MMC treatment. When recalculating foci data regarding the percentage of responding cells (53BP1: $\geqslant 5$ foci/nucleus, RAD51: $\geqslant 2$ foci/nucleus), no statistically significant differences were observed except for a small, namely 7% decrease ($P=0.0302$) of 53BP1-positive cells 6 h post-MMC in the breast cancer patients with mutated *PALB2* versus wild-type *PALB2* controls.

In another approach to unravel the molecular components involved in the DSB repair pathway shift in *PALB2*–mutated individuals, we used western blotting to quantify the phosphorylated repair components indicating DNA damage and repair intermediates, respectively. The damage marker γH2AX detects different types of lesions including stalled replication forks,[45] which accumulate after MMC treatment. P-RPA represents a marker of DSB end processing.[44] We performed at least two independent immunoblotting experiments for each of the LCLs from Finnish donors, normalized antigen-specific signals with the loading control and the internal wild-type reference BR-0968 each, and compared values for the wild-type cohort versus *PALB2*-mutated healthy individuals and breast cancer patients (Figure 5, western blots for individual LCLs in Supplementary Figure 3).

Regarding γH2AX, we observed a trend towards decreased signals in untreated LCLs from mutation carriers with breast cancer down to 41% of the level in the wild-type cohort, which was not seen for the healthy mutation carrier LCLs (Figure 5). Comparison of mean P-RPA (and RPA) band intensities failed to detect major differences between the cohorts. Finally, we investigated endogenous protein levels of key factors implicated in pathway choice decisions. Thus, we examined the important regulator of DSB signaling 53BP1, which promotes NHEJ and antagonizes homologous repair, MRE11, the nuclease component of the DSB recognizing and end processing MRE11-RAD50-Nibrin complex as well as the downstream nuclease CtIP, PARP1, which has been implicated in alternative NHEJ, and RAD51 the central recombinase in HR.[42,46] Interestingly, we observed a 2.3-fold increase of 53BP1 protein levels in the cohort of healthy mutation carriers compared with the wild-type cohort that was lost in the *PALB2*-mutated breast cancer patients (Figure 5). For comparison, none of the other proteins (MRE11, PARP1, RAD51, CtIP) showed quantitative changes. Suggesting posttranslational stabilization of 53BP1 in *PALB2*-mutated healthy individuals versus breast cancer patients, we observed no change and a 53BP1 decrease, respectively, following exposure to the protein biosynthesis inhibitor Cycloheximide (Supplementary Figure 4a). Consistent with 53BP1's proposed role,[46] we found a statistically significant decrease of NHEJ upon *53BP1* knockdown in *PALB2* mutation carriers with and without breast cancer (Supplementary Figure 4b). MMEJ was dependent on 53BP1 only in breast cancer patients. For comparison, inactivation/knockdown of the key factors of HR (RAD51) and SSA (RAD52) caused increased and decreased SSA, respectively, in cells from wild-type *PALB2* control individuals (Supplementary Figure 5). Upon RAD52 knockdown, diminished SSA (and MMEJ, also called micro-SSA) was also noticeable in cells from the healthy *PALB2* mutation carrier, but not from the breast cancer patient of the same family. Therefore, RAD52-independent mechanisms promote SSA in *PALB2*-mutated cells from the breast cancer patients.

DISCUSSION

The EMBRACE study demonstrated the dramatic effect of modifier genes on the cancer risk of *BRCA2* mutation carriers.[47] These results underscore the need for comprehensive parameters, which describe the combined breast cancer risk of high-penetrance susceptibility genes in the individual's genetic background. In our previous study, we demonstrated an association between distinct DSB repair activities and breast cancer risk.[40] The heterozygous

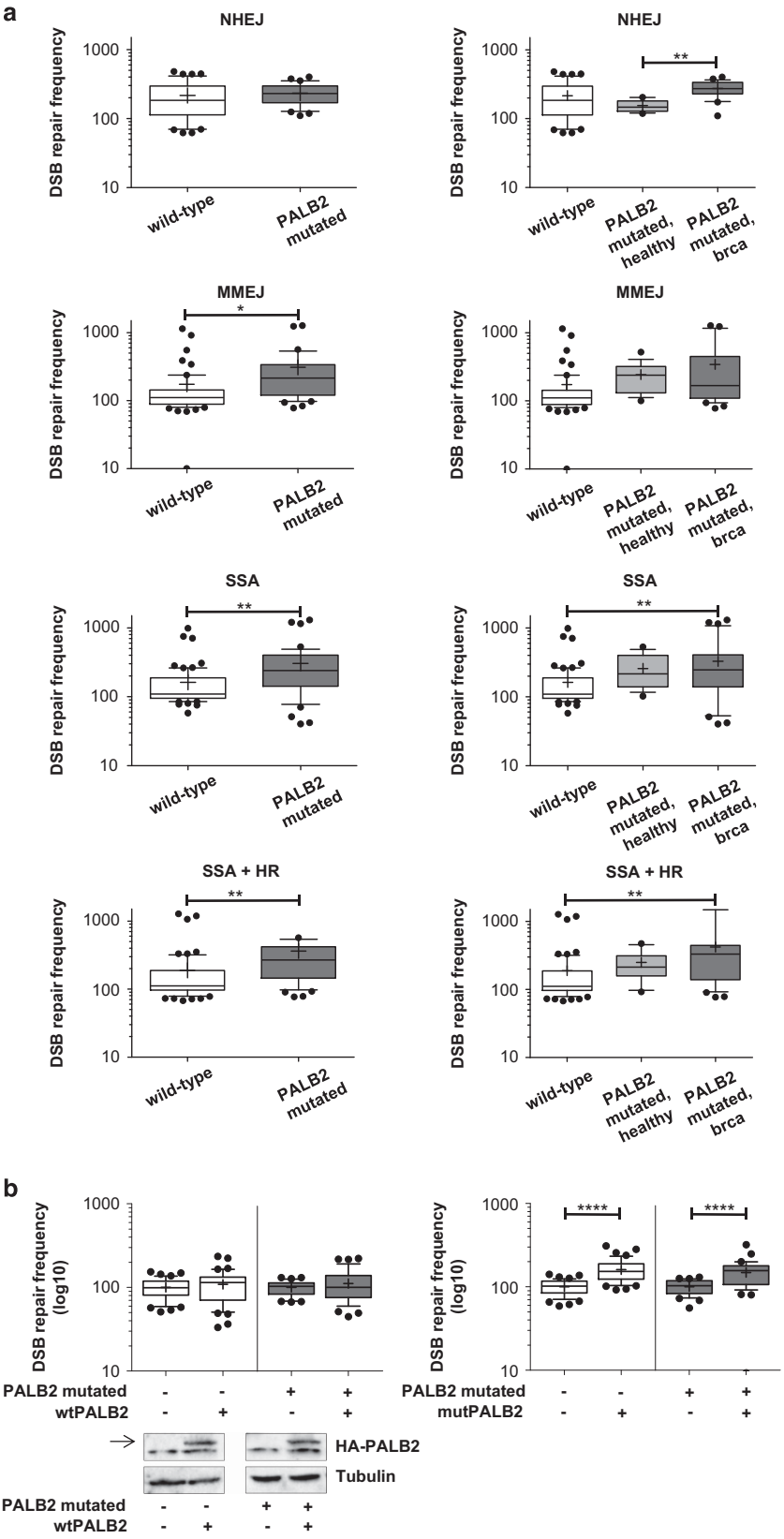

Finnish *PALB2* c.1592delT founder mutation leads on average to a sixfold increase in breast cancer risk.[9] In our study, we elucidated the DSB repair phenotype of female *PALB2* c.1592delT mutation carriers as compared with wild-type individuals.

The heterozygous *PALB2* germline mutation most prominently caused increases in the error-prone activities MMEJ (2- to 10-fold) and even more significantly in SSA/SSA+HR (2- to 11-fold) as determined via analysis of cohorts and comparison of individual carrier LCLs versus wild-type reference. These data indicated a mixed phenotype of *PALB2* mutation carrier cells as compared with heterozygously *BRCA1*-mutated cells, which had correspondingly been characterized by 3- to 16-fold elevated MMEJ and heterozygously *BRCA2*-mutated cells with threefold increased SSA activities.[36] This mixed cellular phenotype reflects the physical interactions of PALB2 connecting BRCA1 and BRCA2.[19–21] As previously observed with heterozygously *BRCA1*- and *BRCA2*-mutated cells,[36] HR was not consistently found to be impaired in heterozygously mutated *PALB2* cells. This finding can partially be explained by the fact that HR frequencies were closer to the detection limit, which made HR and a further decrease of this activity more difficult to detect. On the other hand, a fivefold HR decrease was in fact measured in one *PALB2*-mutated cell type (Table 1). Another explanation could be that alternative HR repair mechanisms engaging RAD52 or involving template switch or break-induced replication, which are not or less sensitive to lack of RAD51 and BRCA2,[48–50] became prevalent in *PALB2* mutation carrier cells. Finally, the possibility remains that the *PALB2*

Table 2. PARP inhibitor sensitivities of LCLs with mutations in *BRCA2* or *PALB2* versus wild-type

Cell line	*Genotype*	*Health status*	*IC50*[a]	P-*value*[b]
TK6	Wild-type	Healthy	76	–
HA238	*BRCA2* (c.5946delCT/wt)	brca	45	0.0464
GM13023A	Biallelic *BRCA2* mutation	Fanconi anemia	12	< 0.0001
BR-0968	Wild-type	Healthy	39	
BR-0778			23	0.2130
BR-0781			57	0.0556
BR-1016			47	0.4858
BR-1017			26	0.5245
BR-1023			38	0.7369
BR-0954	*PALB2* (c.1592delT/wt)	Healthy	41	0.6937
BR-0967			38	0.6241
BR-0724		brca	45	0.7500
BR-0736			36	0.8263
BR-0737			24	0.4956
BR-0760			16	0.0469
BR-0970		brca+therapy	6	0.0432

Abbreviations: brca, breast cancer patient; brca+therapy, breast cancer patient undergoing cytostatic therapy; LCLs, lymphoblastoid cell lines. LCLs were treated with increasing concentrations of 1,5-isoquinolinediol (IQD; 2 μM–2 mM). Cell viability was assessed using MTT assay as described in the legend to Figure 3. IC50 values (μM) were determined from 4 to 18 survival curves and statistical significance calculated using F-test of Log IC50 with software GraphPad Prism version 5.04 (numbers of survival curves: BR-0954 6, BR-0967 4, BR-0724 6, BR-0736 6, BR-0737 8, BR-0760 6, BR-0970 4, BR-0778 10, BR-0781 10, BR-1016 6, BR-1017 6, BR-1023 4 and reference BR-0968 18)). *P*-values of differences between IC50 values determined in parallel were calculated for *BRCA2*-mutated LCLs versus for wild-type LCL TK6 and for *PALB2*-mutated LCLs versus for wild-type reference LCL BR-0968. [a]Sensitivity to PARP inhibitor IQD treatment (exposure to 2 μM–2 mM for 6 days) was assessed by calculating IC50 values (μM) from 4 to 18 survival curves by use of the software GraphPad Prism version 5.04. [b]*P*-values of differences between IC50 values determined in parallel were calculated for *BRCA2*-mutated LCLs versus for wild-type LCL TK6 and for *PALB2*-mutated LCLs versus for wild-type reference LCL BR-0968.

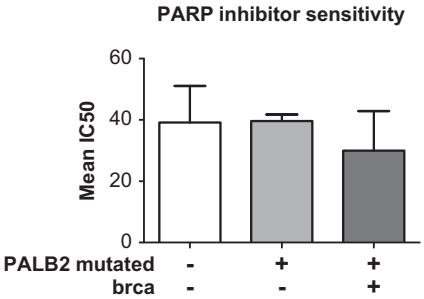

Figure 3. Cohort analysis of PARP inhibitor sensitivities. To determine the cell viability after treatment with the PARP inhibitor 1,5-isoquinolinediol (IQD), increasing IQD concentrations (2 μM-2 mM) were applied. Media were replaced with fresh media including the corresponding IQD concentrations every second day. Cell viability was measured using MTT assay. Mean IC50 values (μM) were determined from 4 to 18 survival curves per LCL and statistical significances calculated using F-test of Log IC50 with software GraphPad Prism version 5.04. The mean IC50 values were visualized as columns in three cohorts, encompassing six LCLs with wild-type *PALB2* (white columns), two LCLs derived from healthy *PALB2* mutation carriers (light gray columns), and four LCLs from *PALB2* mutation carriers with breast cancer (dark gray columns). Bars show s.d. ($n = 2–6$).

Figure 2. Cohort analysis of DSB repair pathway usage in wild-type and heterozygously *PALB2*-mutated individuals with and without breast cancer. (**a**) DSB repair as a function of the endogenous PALB2 status. LCLs from six wild-type *PALB2* individuals (white columns) and six *PALB2* c.1592delT mutation carriers (dark gray columns, left panel), among those two from healthy individuals (light gray columns, right panel) and four from breast cancer patients (dark gray columns, right panel), were transfected with reporter constructs for analysis of NHEJ, MMEJ, SSA and SSA+HR and repair frequencies determined as described in the legend to Figure 1. Frequencies relative to the reference cell line BR-0968 with wild-type *PALB2* (100%) were determined in 6–36 measurements (average of absolute values corresponding to 100%: NHEJ: 2.9×10^{-3}; MMEJ: 5.2×10^{-4}; SSA: 2.3×10^{-3}; SSA+HR: 2.4×10^{-3}). Data are shown in box plots including mean value (cross) and median (line), 95% confidence interval (CI). Statistical analyses with SPSS were performed using general linear mixed models with mutation status (wild-type or *PALB2*-mutated, left panel) or mutation and health status (wild-type, *PALB2*-mutated and healthy, *PALB2*-mutated and breast cancer; right panel) as fixed factor and date of the experiment as random factor; asterisks indicate a statistically significant difference. (**b**) DSB repair as a function of the exogenous PALB2 status. LCLs from five to six wild-type *PALB2* individuals (except BR-1023 for wild-type PALB2 expression, white columns) and all six *PALB2* c.1592delT mutation carriers not undergoing therapy (gray columns) were transfected with the plasmid mixture for analysis of SSA+HR plus expression plasmid for wild-type PALB2 (wtPALB2), the mutated variant (mutPALB2) or empty vector. DSB repair frequencies were determined as described in (**a**). Mean DSB repair frequencies of each cell line transfected with the empty vector were set to 100%. Data are shown in box plots including mean value (cross) and median (line), 95% CI. Statistically significant differences were calculated by SPSS using Mann–Whitney U test. Asterisks indicate a statistically significant difference. Expression of exogenous PALB2 proteins in LCLs was verified by immunoblotting of lysates with antibody directed against the protein-tag (representatively shown for one wild-type control and one mutation carrier LCL expressing HA-tagged wild-type PALB2; an arrow marks the band specific for HA-tagged PALB2). α-Tubulin was used as the loading control.

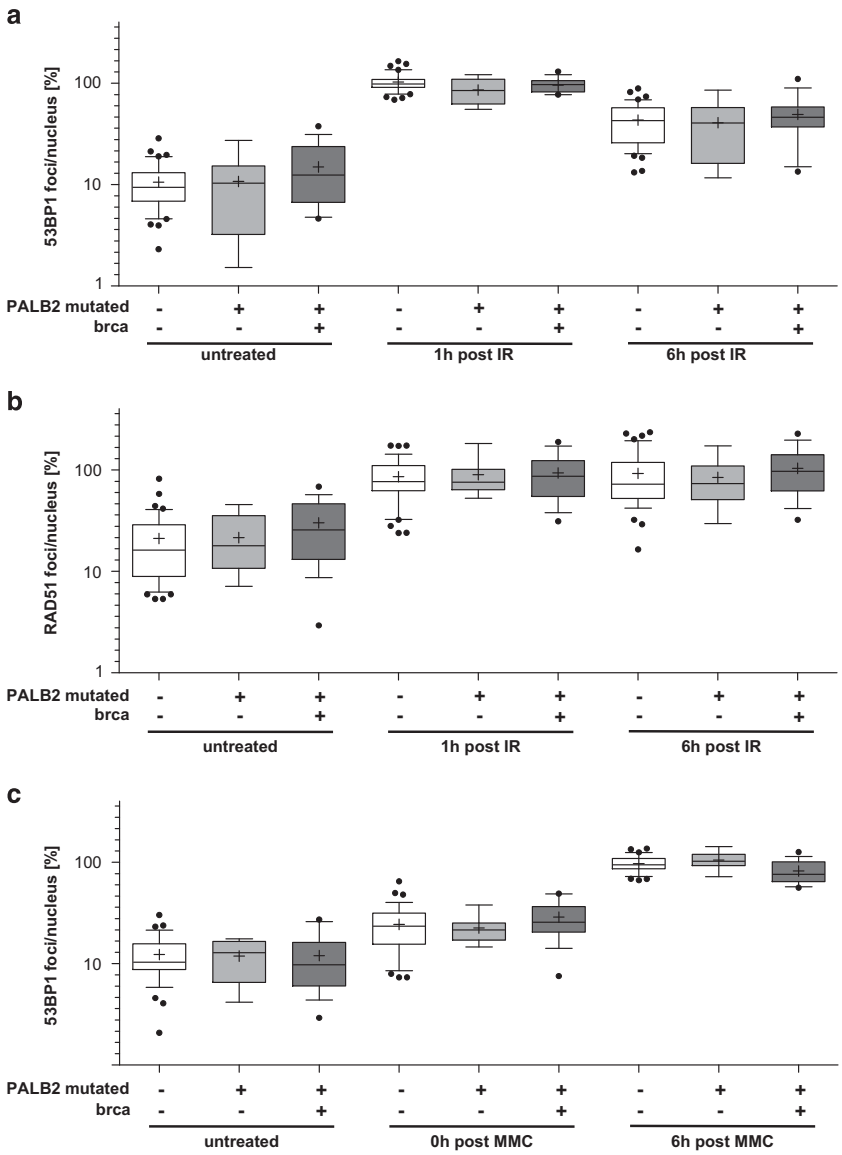

Figure 4. Cohort analysis of DNA damage signals based on immunofluorescence microscopy. DNA damage was induced by ionizing radiation (IR, 2 Gy) (**a**, **b**) or with MMC (2.6 μM, 45 min) (**c**) followed by reincubation in fresh medium. Focal accumulation of the damage marker 53BP1 (**a**, **c**) or the recombinase RAD51 (**b**) in the nuclei were analyzed at the indicated time points post treatment by immunofluorescence microscopy (IR: 1 h (0.5–1.0 h), 6 h; MMC: 0 h, 6 h). Immunolabeled foci from two slides and two independent experiments each were scored by automated quantification of 25 nuclei for each slide. Maximum mean scores for the wild-type LCL BR-0968 were set to 100% in each experiment and relative percentages calculated for each single value (corresponding to one slide). Data are shown in box plots ($n = 8–40$) including mean value (cross) and median (line), 95% confidence interval. Statistical analyses with SPSS were performed using general linear models with mutation and health status (wild-type, *PALB2*-mutated and healthy, *PALB2*-mutated and breast cancer) and treatment group (untreated control, 0 or 1 h post treatment, 6 h post treatment) as fixed factor. Wild-type *PALB2*, white columns; healthy *PALB2*-mutated carriers, light gray columns; *PALB2*-mutated breast cancer patients, dark gray columns. (**a**) 53BP1 foci analysis after IR. (**b**) RAD51 foci analysis after IR. (**c**) 53BP1 foci analysis after MMC treatment.

(c.1592delT/wt) status is associated with haploinsufficiency regarding the suppression of error-prone DSB repair activities but with haplosufficiency regarding stimulation of RAD51-dependent HR. In agreement with this concept, we monitored normal RAD51 foci kinetics in most of the *PALB2* mutation carrier cell lines. Moreover, the accumulation and decline of DSBs as indicated by 53BP1 foci after irradiation or MMC treatment were similar in wild-type and mutated cell types. A clue to haploinsufficiency regarding the suppression of error-prone repair could be that the truncated *PALB2* c.1592delT gene product is highly unstable. Upon overexpression, truncated PALB2 may also exert a dominant-negative influence via the N-terminal BRCA1-binding site[21,32] as suggested from the observed increase in error-prone DSB repair. BRCA1 via its association with CtIP is involved in the pathway choice, as it promotes DSB end resection and therefore homologous repair rather than classical NHEJ.[26] In normal cells, BRCA1 promotes RAD51-dependent HR via its association with PALB2. Blocking PALB2 but not CtIP interactions will favor RAD51-independent homologous repair like SSA and other unscheduled processes requiring ssDNA overhangs like MMEJ.

Measurements of total NHEJ, encompassing canonical and alternative activities, revealed augmented usage of NHEJ in the majority of *PALB2* mutation carrier cell lines, however, also in several wild-type *PALB2* LCLs. Previous data indicated the involvement of not only MMEJ but also SSA in generating chromosomal rearrangements that can lead to malignancies.[51]

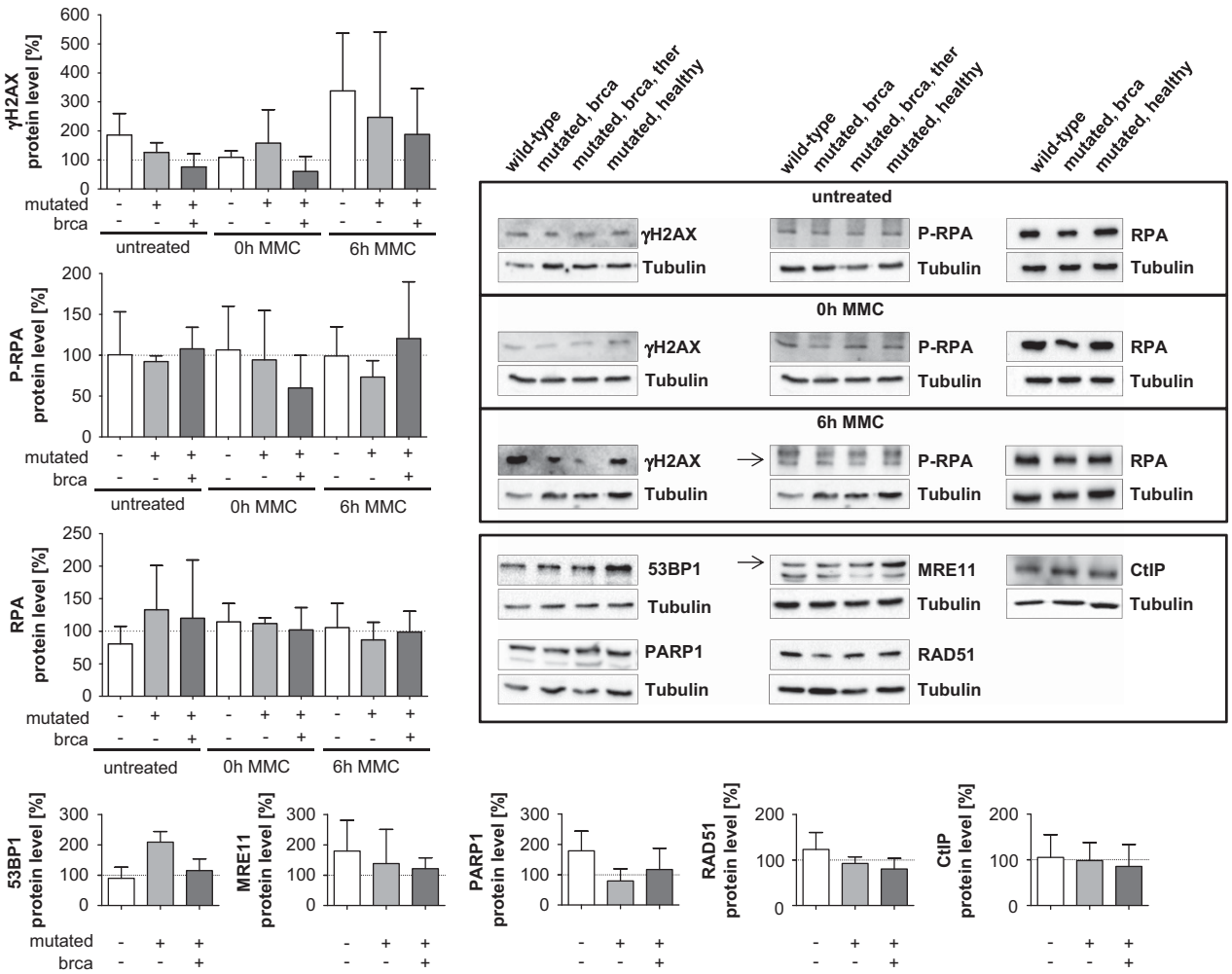

Figure 5. Cohort analysis of DSB repair protein levels. Endogenous levels of DSB repair proteins in LCLs from twelve Finnish donors were visualized by immunoblotting of lysates containing 50 μg protein per sample with antibodies directed against γH2AX, P-RPA, RPA, 53BP1, MRE11, PARP1, RAD51and CtIP. α-Tubulin was used as loading control. Samples were collected from untreated LCLs (basal level), immediately (0 h) or 6 h after treatment with MMC (2.6 μM, 45 min). Two independent immunoblotting experiments were performed for each cell line. Band intensities were quantified and individually corrected with the loading control. Arrows indicate quantified bands in case of several bands. The wild-type *PALB2* LCL BR-0968 was used as reference on each immunoblot and set to 100%. Columns represent the mean relative changes (versus BR-0968) of protein levels per tested cell line from three cohorts, namely six LCLs with wild-type *PALB2* (white columns), two LCLs derived from healthy *PALB2* mutation carriers (light gray columns) and four LCLs from *PALB2* mutation carriers with breast cancer (dark gray columns). Bars show s.d. ($n = 2–6$). brca+ther, breast cancer patient undergoing cytostatic therapy.

Notably, a reduced capacity to reactivate stalled replication forks as well as chromosomal aberrations including complex rearrangements that are mechanistically linked with homologous repair activities have been observed in *PALB2* c.1592delT mutation carriers.[32] Fully error-prone DSB repair activities (MMEJ, SSA) were increased in all studied *PALB2* mutation carrier LCLs except for two from breast cancer patients. One of those two cell lines, namely from the patient undergoing therapy, was particular as it did not match the DSB repair pattern of the other *PALB2*-mutated LCLs (neither increase of NHEJ, MMEJ, SSA and/or SSA+HR but decrease of HR) which might indicate interference of cytostatic treatment with the DSB response. When disregarding this cell line, augmentation of MMEJ and SSA each associated with five out of six of the *PALB2*-mutated LCLs, however, also detected one (MMEJ) and two out of six (SSA), respectively, wild-type *PALB2* LCLs (including BR-0968, Table 1). Notably, the relative increase detected in the few wild-type LCLs was also less pronounced, namely less than 2-fold for MMEJ and 2- to 5-fold for SSA versus in *PALB2*-mutated cells 2- to 10-fold and 2- to 8-fold, respectively.

When performing cohort analysis, we confirmed the increase of MMEJ and SSA in the *PALB2* c.1592delT mutation carriers. Subgroup analysis further revealed a rise of SSA in the breast cancer patients compared with wild-type controls and of NHEJ in the breast cancer patients compared with the healthy mutation carriers. Considering that *PALB2* is a FA gene,[13,14] our finding on NHEJ is in line with earlier reports demonstrating that FA cells exhibit elevated NHEJ.[52] Hence, mutation carriers with breast cancer more frequently used error-prone DSB repair pathways, which are known to induce genomic instability, and therefore are likely to have accelerated malignancy formation. We propose that additional genetic alterations in this group of *PALB2* mutation carriers exacerbated the HR defect and usage of error-prone DSB repair pathways and thus breast cancer risk.

The principle of synthetic lethality has been pursued in PARP inhibitor trials targeting HR-defective tumors.[43] In line with the proficiency in HR of the heterozygous *PALB2* c.1592delT mutation carriers, we found increased sensitivity to the drug only in two *PALB2* mutation carrier cell lines derived from breast cancer

patients. One possibility to explain PARP inhibitor sensitivity in these two but not the other LCLs could be that additional genetic or epigenetic alterations might have exacerbated the defect.

Of interest regarding a potential role of the *PALB2* c.1592delT mutation in the response of breast cancer patients to conventional chemotherapies, we observed increased levels of 53BP1 in healthy *PALB2* c.1592delT mutation carriers but not in breast cancer patients. Together with RIF1 and PTIP, 53BP1 was reported to prevent unscheduled resection of DSBs, particularly in BRCA1-deficient cells.[46] Consistent with a role of 53BP1 in NHEJ,[46] *53BP1* knockdown downregulated NHEJ in both the cohort of *PALB2*-mutated healthy individuals as well as in breast cancer patients. However, 53BP1 was limiting for MMEJ in breast cancer patients in particular. Our results further suggested that RAD52 may contribute to SSA and MMEJ in healthy mutation carriers, while RAD52-independent SSA and MMEJ mechanisms[53] may have a more important role in patients. Altogether, we found differential involvement of DSB repair components in compensatory error-prone DSB repair in healthy mutation carriers and breast cancer patients. Importantly, in triple-negative breast cancer, which is frequently associated with a nonfunctional BRCA1 and FA pathway, 53BP1 was found to be downregulated in a subset of the cases associated with reduced therapeutic responsiveness and probability of survival.[54,55] Therefore, our findings also impact on the design of personalized treatment regimens of breast cancer patients with a *PALB2* c.1592delT mutation.

Functional assays gradually enter the clinic to contribute to the classification of variants of uncertain significance in *BRCA1* and *BRCA2*.[56,57] Our previous work has taken functional analysis one step further demonstrating DSB repair dysregulation directly in immortalized and primary cells derived from individuals with hereditary breast cancer risk.[36] In this study, we observed haploinsufficiency in *PALB2* c.1592delT mutation carriers (without therapy) regarding the suppression of error-prone DSB repair, however, not regarding HR changes, RAD51 filament assembly or PARP inhibitor sensitivity. Thus, mutation carriers exhibited significantly increased MMEJ and SSA activities. This shift in DSB repair pathway usage is particularly detrimental in the context of the aberrant replication phenotype observed previously in the same *PALB2* c.1592delT mutation cohort cells.[32] We consider the replication stress as a source of DSBs in combination with the increased error-prone DSB repair described here sufficient to explain the increase in genetic aberrations including complex chromosomal rearrangements in *PALB2* c.1592delT mutation carrier cells.[32] The difference in DSB repair pathway usage was even more significant in the *PALB2* mutation carriers with breast cancer, underscoring the potential of the functional approach to capture additional risk factors. Intriguingly, in the breast cancer patients, we noticed the loss of 53BP1 accumulation, which has prognostic value in triple-negative breast cancer patients. Combining analysis of error-prone DSB repair activities and of 53BP1 levels may contribute to multifactorial models to predict the pathogenicity of individual risk genes, the individual cancer risk and/or therapeutic responses.

MATERIALS AND METHODS

LCLs and cell culturing

LCLs originating from seven female Finnish *PALB2* c.1592delT mutation carriers and six wild-type matched controls (Supplementary Table 1) were provided by the Laboratory of Cancer Genetics and Tumor Biology, University of Oulu, Finland, and described in the study by Nikkilä *et al*.[32] Additional LCLs were HA238 with heterozygously mutated *BRCA2* (provided by Medical University Hannover, Germany), GM13023A with biallelic *BRCA2/FANCD1*-mutation (purchased at Coriell Institute, Camden, NJ, USA), and the control LCL TK6 (provided by Eppendorf University Clinic, Hamburg, Germany), which were all described in the study by Keimling *et al*.[36] LCLs were cultivated in RPMI 1640 medium (Gibco/Invitrogen, Carlsbad, CA, USA) supplemented with 15% fetal bovine serum (Biochrom, Merck Millipore, Darmstadt, Germany) and antibiotics (Penicillin-Streptomycin-Glutamine, Gibco/Invitrogen). Experiments were performed in antibiotic-free media with 1.5% L-glutamine (Gibco/Invitrogen). All LCLs were tested negative for *Mycoplasma* contamination.

DSB repair analysis

LCLs were analyzed in sets, whereby the reference LCL BR-0968 was included in all sets. The capacity and quality of DSB repair was analyzed by use of a previously described *EGFP*-based test system.[39] For this purpose, LCLs were electroporated with a plasmid mixture containing 10 μg of one of the DSB repair substrates (EJ5SceGFP, EJ-EGFP, 5'EGFP/HR-EGFP, HR-EGFP/3'EGFP, HR-EGFP/5'EGFP)[39,58] together with 10 μg of the meganuclease expression plasmid pCMV-I-*Sce*I, and 10 μg of the filler plasmid pBS by use of a Gene Pulser with Pulse Controller from Bio-Rad (München, Germany) at 220 V and 1050 μF. To specify transfection efficiencies, wild-type *EGFP* expression plasmid was used instead of pBS in parallel samples each. Fourty-eight hours post transfection, green fluorescent cells containing reconstituted EGFP were quantified by flow cytometry using FACSCalibur (Becton-Dickinson, Heidelberg, Germany). Laser excitation was effected at 488 nm and gated life cells (side scatter/forward scatter dot plot) were detected in the FL1/FL2 channel. The recombination frequency was calculated by green fluorescent cells per life cell count divided by the transfection efficiency per life cell count. In experiments analyzing exogenous PALB2 protein, we added 40 μg of the POZ-PALB2 expression plasmid for HA-tagged wild-type PALB2[41] or of the expression plasmid for the tagged truncated variant encoded by *PALB2* c.1592delT (Origene, Rockville, MD, USA). To silence 53BP1 during DSB repair measurements, we included 40 μg of two specific pRS-based shRNA expression plasmids (Origene) into the mixture, to express RAD51SM pcDNA3.1-Rad51SM, to silence RAD52 pSUPER-RAD52.

Our study followed the guideline by Guidugli *et al*.[57] of assay development for *BRCA2* mutation carriers. Thus, we used an internal reference, replicated each sample, repeated each experiment at least twice, measured the transfection efficiency and prepared plasmids in batches to assure the same DNA quality. During assay optimization, we added further quality criteria to the present study, namely a minimum transfection efficiency for HR (⩾10%), maximum LCL passage numbers (⩽25) and performed the whole study in a blinded manner.

Immunofluorescence microscopic analysis

LCLs were exposed to 2 Gy of ionizing radiation (Cs-137, GSR D1, Gamma-Service Medical GmbH, Leipzig, Germany) or treated with MMC (2.6 μM; Sigma-Aldrich, Steinheim, Germany) for 45 min, reincubated with fresh medium and harvested at the indicated time points post treatment. After cytospinning (Cytospin3 Centrifuge, Shandon, Bohemia, NY, USA) at 28 × *g* for 5 min on slides covered by poly-L-Lysine (Sigma-Aldrich), cells were, depending on the specific antibody applied, pre-extracted or fixed immediately with 3.7% formaldehyde followed by permeabilization with 0.5% TritionX-100. Five percent Goat Serum (Invitrogen, Karlsruhe, Germany) in phosphate-buffered saline was utilized for blocking. Primary antibodies used were polyclonal antibodies targeting 53BP1 (NB100-304, Novus Biologicals, Littleton, CO, USA) and RAD51 (H-92, Santa Cruz Biotechnology, Heidelberg, Germany); secondary antibody was AlexaFluor555-labeled (Invitrogen). Stained cells were mounted either with Dabco (1,4-Diazabicyclo[2.2.2]-octane, Sigma-Aldrich) and Mowiol (MOWIOL^R 4–88 Reagent, Calbiochem, Merck Millipore) after staining with DAPI (4′,6-Diamidino-2-phenylindole dihydrochloride, Sigma-Aldrich) or Vectashield containing DAPI (Vector laboratories, Burlingame, CA, USA). Focal accumulation of 53BP1 and RAD51 in the nuclei was analyzed in a time-dependent manner using an Olympus BX51 epifluorescence microscope with ×100 oil immersion objective fitted with cooled charge-coupled device camera (Colorview 12, Olympus, Tokyo, Japan) and Cell^F imaging software version 2.5 (Olympus Soft Imaging Solutions, Münster, Germany). On each experimental day, 50 nuclei from two independent slides were analyzed. The threshold was maintained throughout one experimental set.

PARP inhibitor sensitivity

To assess the response to the PARP inhibitor 1,5-isoquinolinediol (ENZO, New York, NY, USA), MTT assay was performed as described.[59] One day post seeding, LCLs were treated with different 1,5-isoquinolinediol concentrations from 2 μM to 2 mM 1,5-isoquinolinediol for 6 days.

Western blotting

LCLs were mock-treated or treated with MMC (2.6 μM) for 45 min followed by incubation in fresh media and harvested at the indicated time points. After preparation of the lysates, proteins were electrophoresed by SDS–PAGE and transferred to nitrocellulose or polyvinylidene fluoride membrane. Proteins were detected by the following antibodies recognizing 53BP1 (NB100-304, Novus Biologicals, Cambridge, UK), CtIP (T-16, Santa Cruz Biotechnology, Santa Cruz, CA, USA), MRE11 (NB100-142, M-2; Novus Biologicals), RAD51 (H-92, Santa Cruz Biotechnology), RAD52 (5H9, Abcam, Cambridge, UK), RPA (Ab-2, Calbiochem, Darmstadt, Germany), phospho-RPA (P-RPA; S33, Bethyl Laboratories, Montgomery, TX, USA), PARP1 (#9542, Cell Signalling, Danvers, MA, USA), γH2AX (Clone JBW 301 Ser139, Millipore, Billerica, MA, USA), peroxidase-conjugated HA-tag (3F10, Roche, Mannheim, Germany) and α-Tubulin (ab7291, Abcam). Secondary antibodies were peroxidase-conjugated goat anti-mouse (Thermo Scientific, Waltham, MA, USA), anti-rabbit and anti-goat IgG (Rockland, Gilbertsville, PA, USA). Bands were visualized with Clarity Western ECL Substrate (Bio-Rad Laboratories) by ChemiDoc MP Imaging System and quantified using Image Lab 4.1 (Bio-Rad Laboratories).

Statistical evaluation

The statistical significances of differences for set-wise DSB repair measurements, foci analysis and Spearman correlation were determined by the software GraphPad Prism 5.04 (GraphPad, San Diego, CA, USA). Once statistical significance was established for a data set by Kruskal–Wallis test, non-parametric Mann–Whitney test for unpaired samples was applied. GraphPad Prism 5.04 software was further used to generate cell viability curves, calculate IC50 values and statistical significances of the differences between the IC50 values by Extra sum-of-squares F-test of Log IC50. Cohort analyses of DSB repair pathway usage and DNA damage signals were performed using IBM SPSS Statistics Software package version 21. DSB repair pathway usage was analyzed using a general linear mixed model with mutation/health status as fixed factor and date of experiment as random factor. DNA damage signals were analyzed using general linear models with mutation/health status and treatment group (untreated control, 0 or 1 h post treatment, 6 h post treatment) as fixed factors. *Post hoc* tests were adjusted for multiple comparisons using Bonferroni correction. $*P < 0.05$; $**P < 0.01$; $***P < 0.001$; $****P < 0.0001$.

CONFLICT OF INTEREST

The authors declare no conflict of interest. LW is an inventor of a patent on a test system for determining genotoxicities, which is owned by LW.

ACKNOWLEDGEMENTS

We cordially thank Leena Keskitalo, Annika Väntänen and Meeri Otsukka for the initial preparation and culturing of the Northern Finnish *PALB2* mutation carrier and the matched wild-type healthy control LCLs as well as their shipment to Ulm for the current study. We are grateful to Daniela Salles, Ulm, for experimental help during the initial phase of the project, and Jeremy M Stark, Department of Cancer Biology, Division of Radiation Biology, Beckmann Research Institute of the City of Hope, Duarte, CA, USA, for the NHEJ reporter EJ5SceGFP. This project was supported by the International Graduate School in Molecular Medicine Ulm, Germany (to LW). KO was and JS is a member of the International Graduate School in Molecular Medicine Ulm. RW was supported by the University of Oulu and Biocenter Oulu, the Finnish Cancer Foundation, Sigrid Jusélius Foundation and the Academy of Finland Center of Excellence funding (grant 251314). The funders had no role in study design, data collection and analysis, decision to publish, or preparation of the manuscript.

REFERENCES

1 Heikkinen K, Rapakko K, Karppinen SM, Erkko H, Knuutila S, Lundán T *et al. RAD50* and *NBS1* are breast cancer susceptibility genes associated with genomic instability. *Carcinogenesis* 2006; **27**: 1593–1599.
2 Walsh T, King MC. Ten genes for inherited breast cancer. *Cancer Cell* 2007; **11**: 102–105.
3 McKinnon PJ, Caldecott KW. DNA strand break repair and human genetic disease. *Annu Rev Genomics Hum Genet* 2007; **8**: 37–55.
4 Walsh T, Lee MK, Caseidei S, Thornton AM, Stray SM, Pennil C *et al.* Detection of inherited mutations for breast and ovarian cancer using genomic capture and massively parallel sequencing. *Proc Natl Acad Sci USA* 2010; **107**: 12629–12633.
5 Hucl T, Gallmeier E. DNA repair: exploiting the *Fanconi anemia* pathway as a potential therapeutic target. *Physiol Res* 2011; **60**: 453–465.
6 Meindl A, Ditsch N, Kast K, Rhiem K, Schmutzler RK. Hereditary breast and ovarian cancer: new genes, new treatments, new concepts. *Dtsch Ärztebl Int* 2011; **109**: 323–330.
7 Dumitrescu RG, Cotarla I. Understanding breast cancer risk – where do we stand in 2005? *J Cell Mol Med* 2005; **9**: 208–221.
8 Erkko H, Xia B, Nikkilä J, Schleutker J, Syrjäkoski K, Mannermaa A *et al.* A recurrent mutation in *PALB2* in Finnish cancer families. *Nature* 2007; **446**: 316–319.
9 Erkko H, Dowthy JG, Nikkilä J, Syrjäkkoski K, Mannermaa A, Pylkäs K *et al.* Penetrance analysis of the *PALB2* c.1592delT founder mutation. *Clin Cancer Res* 2008; **14**: 4667–4671.
10 Haanpää M, Pylkäs K, Moilanen JS, Winqvist R. Evaluation of the need for routine clinical testing of *PALB2* c.1592delT mutation in BRCA negative Northern Finnish breast cancer families. *BMC Med Genet* 2013; **14**: 1–6.
11 Rahman N, Seal S, Thompson D, Kelly P, Renwick A, Elliott A *et al. PALB2*, which encodes a BRCA2-interacting protein, is a breast cancer susceptibility gene. *Nat Genet* 2007; **39**: 165–167.
12 Casadei S, Norquist BM, Walsh T, Stray S, Mandell JB, Lee MK *et al.* Contribution of inherited mutations in the BRCA2-interacting protein PALB2 to familial breast cancer. *Cancer Res* 2011; **71**: 2222–2229.
13 Reid S, Schindler D, Hanenberg H, Barker K, Hanks S, Kalb R *et al.* Biallelic mutations in *PALB2* cause *Fanconi anemia* subtype *FA-N* and predispose to childhood cancer. *Nat Genet* 2007; **39**: 162–164.
14 Xia B, Dorsman JC, Ameziane N, de Vries Y, Rooimans MA, Sheng Q *et al. Fanconi anemia* is associated with a defect in the BRCA2 partner PALB2. *Nat Genet* 2007; **39**: 159–161.
15 Tischkowitz M, Xia B. *PALB2/FANCN*: recombining cancer and *Fanconi anemia*. *Cancer Res* 2010; **70**: 7353–7359.
16 Thompson LH, Hinz JM. Cellular and molecular consequences of defective *Fanconi anemia* proteins in replication-coupled DNA repair: mechanistic insights. *Mutat Res* 2009; **668**: 54–72.
17 Currall B, Chiangmai C, Talkowski ME, Morton CC. Mechanisms for structural variation in the human genome. *Curr Genet Med Rep* 2013; **1**: 81–90.
18 Ho TV, Schärer OD, Translesion DNA. Synthesis polymerases in DNA interstrand crosslink repair. *Environ Mol Mutagen* 2002; **51**: 552–566.
19 Xia B, Shen Q, Nakanishi K, Ohashi A, Wu J, Christ N *et al.* Control of BRCA2 cellular and clinical functions by a nuclear partner, PALB2. *Mol Cell* 2006; **22**: 719–729.
20 Zhang F, Ma J, Wu J, Ye L, Cai H, Xia B *et al.* PALB2 links BRCA1 and BRCA2 in the DNA-damage response. *Curr Biol* 2009; **19**: 524–529.
21 Zhang F, Fan Q, Ren K, Andreassen PR. PALB2 functionally connects the breast cancer susceptibility proteins BRCA1 and BRCA2. *Mol Cancer Res* 2009; **7**: 11010–11118.
22 Sy SM, Huen MS, Chen J. PALB2 is an integral component of the BRCA complex required for homologous recombination repair. *Proc Natl Acad Sci USA* 2009; **106**: 7155–7160.
23 Park J-Y, Singh TR, Nassar N, Zhang F, Freund M, Hanenberg H *et al.* Breast cancer-associated missense mutants oft he PALB2 WD40 domain, which directly binds RAD51C, RAD51 and BRCA2, disrupt DNA repair. *Oncogene* 2014; **33**: 4803–4812.
24 Sy SM, Huen MS, Chen J. MRG15 is a novel PALB2-interacting factor involved in homologous recombination. *J Biol Chem* 2009; **284**: 21127–21131.
25 Siaud N, Barbera MA, Egashira A, Lam I, Christ N, Schlacher K *et al.* Plasticity of BRCA2 function in Homologous Recombination: genetic interactions of the PALB2 and DNA binding domain. *PLoS Genet* 2011; **7**: 1–12.
26 Roy R, Chun J, Powell SN. BRCA1 and BRCA2: different roles in a common pathway of genome protection. *Nat Rev Cancer* 2012; **12**: 68–78.
27 Shahid T, Soroka J, Kong EH, Malivert L, McIlwraith MJ, Pape T *et al.* Structure and mechanism of action of the BRCA2 breast cancer tumor suppressor. *Nat Struct Mol Biol* 2014; **21**: 962–968.
28 Dray E, Etchin J, Wiese C, Saro D, Williams GJ, Hammel M *et al.* Enhancement of the RAD51 recombinase activity by the tumor suppressor PALB2. *Nat Struct Mol Biol* 2010; **17**: 1255–1259.
29 Petermann E, Orta ML, Issaeva N, Schultz N, Helleday T. Hydroxyurea-stalled replication forks become progressively inactivated and require two different RAD51-mediated pathways for restart and repair. *Mol Cell* 2010; **37**: 492–502.
30 Schlacher K, Christ N, Siaud N, Egashira A, Wu H, Jasin M. Double-strand break repair-independent role for BRCA2 in blocking stalled replication fork degradation by MRE11. *Cell* 2011; **145**: 529–542.
31 Schlacher K, Wu H, Jasin M. A distinct replication fork protection pathway connects Fanconi anemia tumor suppressors to RAD51-BRCA1/2. *Cancer Cell* 2012; **22**: 106–116.
32 Nikkilä J, Parplys AC, Pylkäs K, Bose M, Huo Y, Borgmann K *et al.* Heterozygous mutations in PALB2 cause DNA replication and damage response defects. *Nat Commun* 2013; **4**: 2578.

33 Murphy AK, Fitzgerald M, Ro T, Kim JH, Rabinowitsch AI, Chowdhury D *et al.* Phosphorylated RPA recruits PALB2 to stalled DNA replication forks to facilitate fork recovery. *J Cell Biol* 2014; **206**: 493–507.
34 Riballo E, Kühne M, Rief N, Doherty A, Smith GC, Recio MJ *et al.* A pathway of double-strand break rejoining dependent upon ATM, artemis, and proteins locating to γ-H2AX foci. *Mol Cell* 2004; **16**: 715–724.
35 Huertas P. DNA resection in eukaryotes: deciding how to fix the break. *Nat Struct Mol Biol* 2010; **17**: 11–16.
36 Keimling M, Volcic M, Csernok A, Wieland B, Dörk T, Wiesmüller L. Functional characterization connects individual patient mutation in ataxia telangiectasia mutated (*ATM*) with dysfunction of specific DNA double-strand break-repair signaling pathways. *FASEB J* 2011; **25**: 1–16.
37 Byrnes GB, Southey MC, Hopper JL. Are the so-called low penetrance breast cancer genes, *ATM*, *BRIP1*, *PALB2* and *CHEK2*, high risk for women with strong family histories? *Breast Cancer Res* 2008; **10**: 208.
38 Antoniou AC, Casedei S, Heikkinen T, Barrowdale D, Pylkäs K, Roberts J *et al.* Breast cancer risk in families with mutations in *PALB2*. *N Engl J Med* 2014; **371**: 497–506.
39 Akyüz N, Boehden GS, Süsse S, Rimek A, Preuss U, Scheidtmann KH *et al.* DNA substrate dependence of p53-mediated regulation of double-strand break repair. *Mol Cell Biol* 2002; **22**: 6306–6317.
40 Keimling M, Deniz M, Varga D, Stahl A, Schrezenmeier H, Kreienberg R *et al.* The power of DNA double-strand break (DSB) repair testing to predict breast cancer susceptibility. *FASEB J* 2012; **26**: 1–15.
41 Böhringer M, Obermeier K, Griner N, Waldraff D, Dickinson E, Eirich K *et al.* siRNA identifies differences in the *Fanconi anemia* pathway in BALB/c-*Trp*53+/- with susceptibility versus C57BL/6-*Trp*53+/- mice with resistance to mammary tumors. *Oncogene* 2013; **32**: 5458–5470.
42 De Vos IM, Schreiber V, Dantzer F. The diverse roles and clinical relevance of PARPs in DNA damage repair: current state of the art. *Biochem Pharmacol* 2012; **84**: 137–146.
43 Do K, Chen AP. Molecular pathways: targeting PARP in cancer treatment. *Clin Cancer Res* 2012; **19**: 977–984.
44 Deng X, Prakash A, Dhar K, Baia GS, Colar C, Oakley GG *et al.* Human replication protein A-Rad52-single-stranded DNA complex: stoichiometry and evidence for strand transfer regulation by phosphorylation. *Biochemistry* 2009; **48**: 6633–6643.
45 Gagou ME, Zuazua-Villar P, Meuth M. Enhanced H2AX phosphorylation, DNA replication fork arrest, and cell death in the absence of Chk1. *Mol Biol Cell* 2010; **21**: 739–752.
46 Panier S, Boulton SJ. Double-strand break repair: 53BP1 comes into focus. *Nat Rev* 2014; **15**: 7–18.
47 Mavaddat N, Peock S, Frost D, Ellis S, Platte R, Fineberg E *et al.* Cancer risks for *BRCA1* and *BRCA2* mutation carriers: results from prospective analysis of EMBRACE. *J Natl Cancer Inst* 2013; **105**: 812–822.
48 Constantino L, Sotiriou SK, Rantala JK, Magin S, Mladenov E, Helleday T *et al.* Break-induced replication repair of damaged forks induces genomic duplications in human cells. *Science* 2014; **343**: 88–91.
49 Burkovics P, Sebesta M, Balogh D, Haracska L, Krejci L. Strand invasion by HLTF as a mechanism for template switch in fork rescue. *Nucleic Acids Res* 2014; **42**: 1711–1720.
50 Lok BH, Carley AC, Tchang B, Powell SN. RAD52 inactivation is synthetically lethal with deficiencies in BRCA1 and PALB2 in addition to BRCA2 through RAD51-mediated homologous recombination. *Oncogene* 2013; **32**: 3552–3558.
51 Francis R, Richardson C. Multipotent hematopoietic cells susceptible to alternative double-strand break repair pathways that promote genome rearrangements. *Genes Dev* 2007; **21**: 1064–1074.
52 Bunting SF, Nussenzweig A. Dangerous liaisons: *Fanconi anemia* and toxic non-homologous end joining in DNA crosslink repair. *Mol Cell* 2010; **39**: 164–166.
53 Keka IS, Mohiuddin, Maede Y, Rahman MM, Sakuma T, Honma M *et al.* Smarcal1 promotes double-strand break repair by nonhomologous end-joining. *Nucleic Acids Res* 2015; **43**: 6359–6372.
54 Bouwman P, Aly A, Escandell JM, Pieterse M, Bartkova J, van der Gulden H *et al.* 53BP1 loss rescues *BRCA1* deficiency and is associated with triple-negative and *BRCA*-mutated breast cancers. *Nat Struct Mol Biol* 2010; **17**: 688–695.
55 Ribeiro E, Ganzinelli M, Andreis D, Bertoni R, Giardini R, Fox SB *et al.* Triple negative breast cancers have a reduced expression of DNA repair genes. *PLOS One* 2013; **8**: e66243.
56 Bouwman P, van der Gulden H, van der Heijden I, Drost R, Klijn CN, Prasetyanti P *et al.* A high-throughput functional complementation assay for classification of *BRCA1* missense variants. *Cancer Discov* 2013; **3**: 1142–1155.
57 Guidugli L, Carreira A, Caputo SM, Ehlen A, Galli A, Monteiro AN *et al.* Functional assay for analysis of variants of uncertain significance in BRCA2. *Hum Mutat* 2014; **35**: 151–164.
58 Bennardo N, Gunn A, Cheng A, Hasty P, Stark JM. Limiting the persistence of a chromosomal break diminishes its mutagenic potential. *PLoS Genet* 2009; **5**: 1–14.
59 Ireno IC, Wiehe RS, Stahl AI, Hampp S, Aydin S, Troester MA *et al.* Modulation of the poly(ADP-ribose)polymerase inhibitor response and DNA recombination in breast cancer cells by drugs affecting endogenous wild-type p53. *Carcinogenesis* 2014; **35**: 2273–2282.

Supplementary Information accompanies this paper on the Oncogene website (http://www.nature.com/onc)